Generation of pseudonondiffracting optical beams with superlattice structures

C. H. Tsou, T. W. Wu, J. C. Tung, H. C. Liang, P. H. Tuan, and Y. F. Chen*

Department of Electrophysics, National Chiao Tung University, Hsinchu, Taiwan
*yfchen@cc.nctu.edu.tw

Abstract: We demonstrate an approach to generate a class of pseudonondiffracting optical beams with the transverse shapes related to the superlattice structures. For constructing the superlattice waves, we consider a coherent superposition of two identical lattice waves with a specific relative angle in the azimuthal direction. We theoretically derive the general conditions of the relative angles for superlattice waves. In the experiment, a mask with multiple apertures which fulfill the conditions for superlattice structures is utilized to generate the pseudonondiffracting superlattice beams. With the analytical wave functions and experimental patterns, the pseudonondiffracting optical beams with a variety of structures can be generated systematically.

OCIS codes: (050.4865) Optical vortices; (050.5982) Photonic crystals; (070.3185) Invariant optical fields.

References and links

1. J. Durnin, "Exact solutions for nondiffracting beams. I. The scalar theory," J. Opt. Soc. Am. A **4**(4), 651–654 (1987).
2. J. Durnin, J. J. Miceli, Jr., and J. H. Eberly, "Diffraction-free beams," Phys. Rev. Lett. **58**(15), 1499–1501 (1987).
3. V. Garcés-Chávez, D. McGloin, H. Melville, W. Sibbett, and K. Dholakia, "Simultaneous micromanipulation in multiple planes using a self-reconstructing light beam," Nature **419**(6903), 145–147 (2002).
4. D. McGloin, V. Garcés-Chávez, and K. Dholakia, "Interfering Bessel beams for optical micromanipulation," Opt. Lett. **28**(8), 657–659 (2003).
5. J. Arlt, V. Garces-Chavez, W. Sibbett, and K. Dholakia, "Optical micromanipulation using a Bessel light beam," Opt. Commun. **197**(4-6), 239–245 (2001).
6. Z. Ding, H. Ren, Y. Zhao, J. S. Nelson, and Z. Chen, "High-resolution optical coherence tomography over a large depth range with an axicon lens," Opt. Lett. **27**(4), 243–245 (2002).
7. C. Yu, M. R. Wang, A. J. Varela, and B. Chen, "High-density non-diffracting beam array for optical interconnection," Opt. Commun. **177**(1-6), 369–376 (2000).
8. Z. Bouchal, "Nondiffracting optical beams-physical properties, experiments, and applications," Czech. J. Phys. **53**(7), 537–578 (2003).
9. M. Boguslawski, P. Rose, and C. Denz, "Increasing the structural variety of discrete nondiffracting wave fields," Phys. Rev. A **84**(1), 013832 (2011).
10. M. Boguslawski, P. Rose, and C. Denz, "Nondiffracting kagome lattice," Appl. Phys. Lett. **98**(6), 061111 (2011).
11. P. Rose, M. Boguslawski, and C. Denz, "Nonlinear lattice structures based on families of complex nondiffracting beams," New J. Phys. **14**(3), 033018 (2012).
12. Y. F. Chen, H. C. Liang, Y. C. Lin, Y. S. Tzeng, K. W. Su, and K. F. Huang, "Generation of optical crystals and quasicrystal beams: Kaleidoscopic patterns and phase singularity," Phys. Rev. A **83**(5), 053813 (2011).
13. A. Kudrolli, B. Pier, and J. P. Gollub, Physica, "Superlattice patterns in surface waves," Physica D **123**(1-4), 99–111 (1998).
14. M. Silber and M. R. E. Proctor, "Nonlinear Competition between Small and Large Hexagonal Patterns," Phys. Rev. Lett. **81**(12), 2450–2453 (1998).
15. H. Arbell and J. Fineberg, "Spatial and Temporal Dynamics of Two Interacting Modesin Parametrically Driven Surface Waves," Phys. Rev. Lett. **81**(20), 4384–4387 (1998).
16. H. J. Pi, S. Park, J. Lee, and K. J. Lee, "Superlattice, Rhombus, Square, And Hexagonal Standing Waves In Magnetically Driven Ferrofluid Surface," Phys. Rev. Lett. **84**(23), 5316–5319 (2000).
17. J. F. Nye and M. V. Berry, "Dislocations in wave trains," Proc. R. Soc. Lond. A Math. Phys. Sci. **336**(1605), 165–190 (1974).
18. M. S. Soskin and M. V. Vasnetsov, "Singular Optics," Prog. Opt. **42**, 219–276 (2001).

#195482 - $15.00 USD Received 8 Aug 2013; revised 16 Sep 2013; accepted 17 Sep 2013; published 25 Sep 2013

1. Introduction

A nondiffracting wave field is comprehended as a monochromatic optical field, whose transverse shape remains invariant in free-space propagation. In 1987, Durnin proposed that the nondiffracting wave fields were exact solutions to the homogeneous Helmholtz equation [1]. Such particular solutions can be described as Bessel functions and are called nondiffracting Bessel beams. The realizable beams that propagate with relatively small divergence angle up to a certain range; they have the finite energy and are known as pseudonondiffracting optical beams. In the same year, Durnin *et al.* [2] first experimentally realized a pseudonondiffracting Bessel beam in a cylindrical coordinates system. Since the breakthrough research by Durnin, nondiffracting Bessel beams have been extensively studied and applied in diverse fields, such as optical manipulation [3–5], optical coherence tomography [6], and optical interconnects [7]. In recent years, scientists, mathematicians, and artists have been fascinated with two-dimensional (2D) kaleidoscopic nondiffracting optical patterns [8]. More recently, realizing nondiffracting optical patterns related to crystalline, quasicrystalline and other ordered structures has become an intriguing issue [9–12].

A 2D superlattice pattern is a spatially periodic structure composed of two or more simple planeforms. Since Kudrolli et al. [13] first observed superlattice patterns in a two-frequency forcing Faraday experiment, the superlattice patterns have been widely studied in the experiments of parametrically driven surface waves [14–16]. The superlattice patterns observed by Kudrolli et al. [13] are formed by the coherent superposition of two hexagonal lattice waves with a relative angle of $2\sin^{-1}\left(1/2\sqrt{7}\right)\approx 22^\circ$. Mathematically, there are numerous relative angles satisfying the condition for generating the superlattice waves from superposing two identical lattice waves. Even so, how to determine the specific relative angles for constructing the superlattice waves has not been explored in detail. Therefore, the determination of relative angles is the first issue for generating pseudonondiffracting optical beams with the superlattice structures.

In this paper, we theoretically derive a general condition for the relative angles to construct the superlattice waves from superposing two identical lattice waves. With the derived formulas for the relative angles, numerous superlattice patterns are numerically demonstrated. To realize the pseudonondiffracting optical beams with superlattice structures, we generate the quasi-plane waves by employing a collimated coherent laser to illuminate a mask with multiple tiny apertures. The positions of the apertures are precisely manufactured with a stencil laser cutting machine to fulfill the condition for generating the superlattice patterns. We also analyze the influence of the aperture size on the formation of the transverse unit cell in the pseudonondiffracting superlattice beam. The experimental results are found to be in a good agreement with the numerical calculations. Furthermore, we manifest the structures of phase singularities for the superlattice patterns. The optical fields with phase singularities, also known as optical vortices, have been studied and generated a lot of interest in recent years [17, 18]. We expect that the pseudonondiffracting superlattice beams with phase singularities can be potentially beneficial to future applications for the optical vortex beams.

2. Theoretical analysis for forming superlattice waves

A 2D lattice wave in polar coordinates (ρ,ϕ) which is formed by the superposition of three, four or six plane waves can be expressed as [12]

$$\psi_q\left(\rho,\phi;\vec{K}_s\right)=\frac{1}{q}\sum_{s=0}^{q-1}e^{i\vec{K}_s\cdot\vec{\rho}}, \tag{1}$$

where $\vec{K}_s=\left(K\cdot\cos\left(2\pi s/q\right),K\cdot\sin\left(2\pi s/q\right)\right)$, $\vec{\rho}=\left(\rho\cdot\cos\left(\phi\right),\rho\cdot\sin\left(\phi\right)\right)$, $\vec{K}_s$ is the wave vector, and q is equal to 3, 4, or 6. Considering the coherent superposition of two identical

#195482 - $15.00 USD Received 8 Aug 2013; revised 16 Sep 2013; accepted 17 Sep 2013; published 25 Sep 2013

lattice waves with a relative angle in the azimuthal direction, we can obtain the superposed waves as

$$\Psi_q\left(\rho,\phi;\vec{K}_s,\Delta_q\right)=\psi_q\left(\rho,\phi;\vec{K}_s\right)+\psi_q\left(\rho,\phi;\vec{K}_s'\right), \tag{2}$$

where $\vec{K}_s'=\left(K\cdot\cos\left[\left(2\pi s/q\right)+\Delta_q\right],K\cdot\sin\left[\left(2\pi s/q\right)+\Delta_q\right]\right)$, and Δ_q is the relative angle between $\vec{K}_s$ and $\vec{K}_s'$. Figure 1(a)-1(c) depicts the wave vectors of the superposed waves with q = 3, 4, and 6, respectively. The solid and dashed vectors represent $\vec{K}_s$ and $\vec{K}_s'$, respectively.

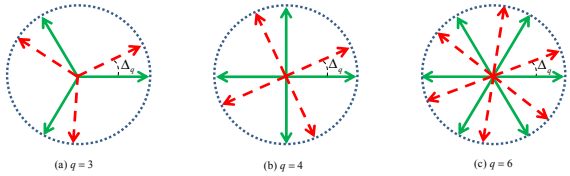

Fig. 1. The schematic diagrams of the wave vectors of the superposed waves $\Psi_q\left(\rho,\phi;\vec{K}_s,\Delta_q\right)$ with (a) q = 3, (b) q = 4, and (c) q = 6.

The superposed waves are spatially periodic when the wave vectors are located on the reciprocal lattice points of the superposed wave fields. In other words, the wave vectors can be expressed as the linear combinations of reciprocal primitive translation vectors. For instance, since the reciprocal primitive translation vectors are orthogonal for q = 4, the wave vectors shown in Fig. 1(b) must be satisfied the following conditions

$$\begin{cases}\vec{K}_s=n_s\cdot\vec{b}_1+m_s\cdot\vec{b}_2\\ \vec{K}_s'=n_s'\cdot\vec{b}_1+m_s'\cdot\vec{b}_2\\ \left|\vec{K}_s\right|=b\sqrt{{n_s}^2+{m_s}^2}=b\sqrt{{n_s'}^2+{m_s'}^2}=\left|\vec{K}_s'\right|\end{cases}, \tag{3}$$

where $\left(n_s,m_s\right)$ and $\left(n_s',m_s'\right)$ are two coprime integer pairs, $\vec{b}_1$ and $\vec{b}_2$ are the reciprocal primitive translation vectors of the spatially periodic superposed waves, and $b=\left|\vec{b}_1\right|=\left|\vec{b}_2\right|$. Combining all conditions of the wave vectors, the most general solutions of n_s' and m_s' are given by

$$\begin{cases}n_s'=m_s\\ m_s'=n_s\end{cases}. \tag{4}$$

Therefore, $\vec{K}_s'$ can be rewritten in terms of n_s and m_s as

$$\vec{K}_s'=m_s\cdot\vec{b}_1+n_s\cdot\vec{b}_2. \tag{5}$$

There are some accidental solutions of n_s' and m_s' which are not included in Eq. (4). Because these cannot be expressed in an analytic form, we focus on the most general solutions given by Eq. (4). As a result, the specific relative angles Δ_q for spatially periodic waves are subject to following the condition

$$\Delta_q=\cos^{-1}\left(\frac{\vec{K}_0\cdot\vec{K}_0'}{\left|\vec{K}_0\right|\left|\vec{K}_0'\right|}\right)=\cos^{-1}\left(\frac{2n_0\cdot m_0}{{n_0}^2+{m_0}^2}\right),\ \text{for } q=4. \tag{6}$$

#195482 - $15.00 USD Received 8 Aug 2013; revised 16 Sep 2013; accepted 17 Sep 2013; published 25 Sep 2013

By utilizing the condition of relative angles, we can generate a class of superposed waves for q = 4 with spatial periodicity. With the wave vectors in terms of the reciprocal primitive translation vectors, the reciprocal lattice constant can be given by

$$b = \left|\vec{b}_1\right| = \left|\vec{b}_2\right| = \frac{K}{\sqrt{{n_0}^2 + {m_0}^2}}, \text{ for } q = 4. \tag{7}$$

Equation (7) indicates that the spatial period becomes longer when the value of $\sqrt{{n_0}^2 + {m_0}^2}$ gets larger. Following an analogous derivation, the criteria for spatial periodicity of superposed waves with q = 3 and 6 can be obtained. Since the scalar product of the reciprocal primitive translation vectors is −1/2 in the cases of q = 3 and 6, the condition of the relative angles leads to the equation

$$\Delta_q = \cos^{-1}\left(\frac{-{n_0}^2 - {m_0}^2 + 4n_0 \cdot m_0}{2\left({n_0}^2 + {m_0}^2 - n_0 \cdot m_0\right)}\right), \text{ for } q = 3 \text{ or } 6, \tag{8}$$

and the reciprocal lattice constant is given by

$$b = \frac{K}{\sqrt{{n_0}^2 + {m_0}^2 - n_0 \cdot m_0}}, \text{ for } q = 3 \text{ or } 6. \tag{9}$$

Consequently, the superlattice waves can be constructed by the superposed waves $\Psi_q\left(\rho, \phi; \bar{K}_s, \Delta_q\right)$ with specific relative angles.

Figures 2(a)-2(c) depict the calculated patterns for the intensity of the superlattice waves $\left|\Psi_q\left(\rho, \phi; \bar{K}_s, \Delta_q\right)\right|^2$ with q = 4. It can be seen that a rich variety of superlattice wave patterns can be constructed by controlling the specific relative angle. The numerical patterns for the intensity of superlattice waves with q = 3 and 6 are shown in Figs. 3(a)-3(c) and Figs. 3(d)-3(f), respectively. These numerical patterns show that the specific relative angle can turn into the main parameter for generating nondiffracting optical superlattice beams. In the following section we present an approach to realize the pseudonondiffracting optical superlattice beams.

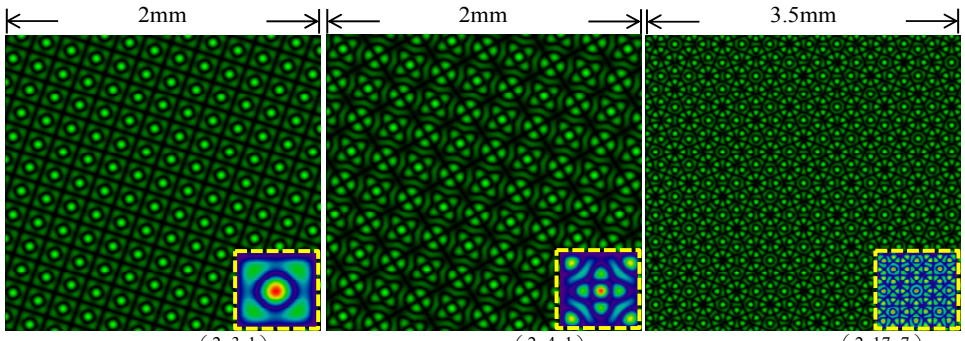

Fig. 2. Numerical patterns for the intensity of the superlattice waves $\left|\Psi_q\left(\rho, \phi; \bar{K}_s, \Delta_q\right)\right|^2$ with $q = 4$.

#195482 - $15.00 USD Received 8 Aug 2013; revised 16 Sep 2013; accepted 17 Sep 2013; published 25 Sep 2013

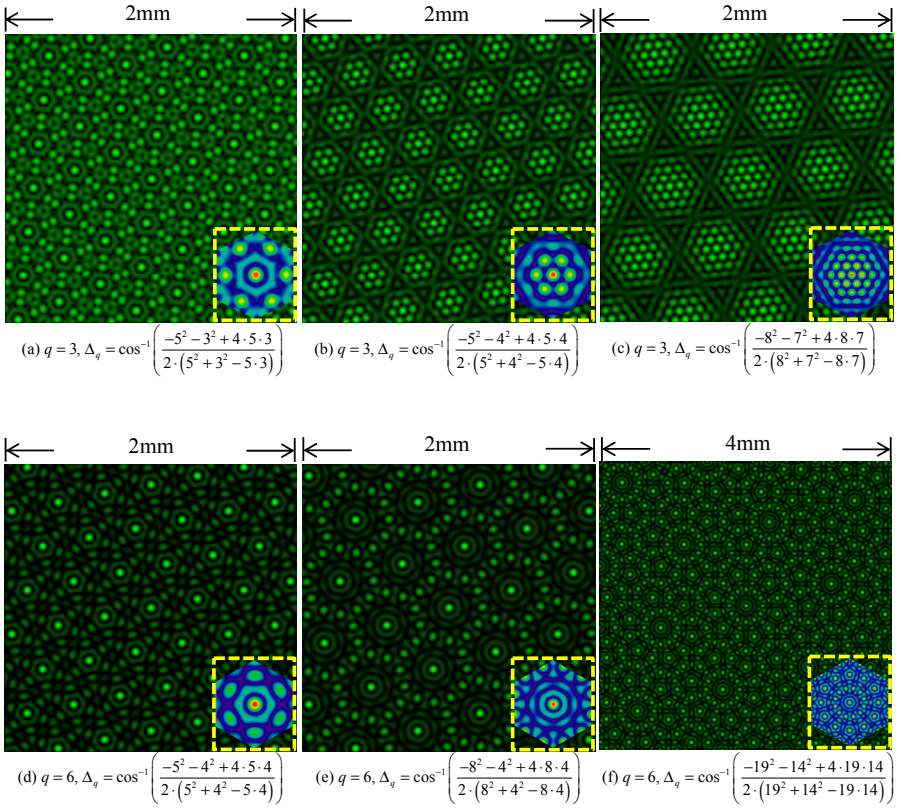

Fig. 3. Numerical patterns for the intensity of the superlattice waves $\left|\Psi_q\left(\rho,\phi;\bar{K}_s,\Delta_q\right)\right|^2$ with (a)-(c) q = 3, and (d)-(f) q = 6.

3. Generation of the pseudonondiffracting optical superlattice beams

A pseudonondiffracting Bessel beam can be generated by an annular slit illuminated with a collimated light and placed in the focal plane in front of a lens [2]. Based on Fourier optics, the relation between the input field $E_i\left(\rho',\phi'\right)$ in the focal plane in front of a lens and the output field $E_o\left(\rho,\phi,z\right)$ behind the lens at a distance z can be expressed as

$$E_o\left(\rho,\phi,z\right)=\frac{-ie^{i\frac{2\pi}{\lambda}(f+z)}}{\lambda f}\iint E_i\left(\rho',\phi'\right)e^{i\frac{2\pi}{\lambda}\frac{\rho'^2}{2f}\left(1-\frac{z}{f}\right)}e^{-i\frac{2\pi\rho\rho'}{\lambda f}\cos(\phi-\phi')}\rho' d\rho' d\phi', \quad (10)$$

where λ is the wavelength of coherent light source, and f is the focal length of the lens. For a pseudonondiffracting Bessel beam, the input field is determined by an infinitesimally thin annulus at $\rho'=R$ expressed as

$$E_i\left(\rho',\phi'\right)=\delta\left(\rho'-R\right), \quad (11)$$

where $\delta(\bullet)$ is the Dirac delta function. A finite-energy pseudonondiffracting Bessel beam requires an annular ring of finite thickness at the input plane. The pseudonondiffracting beams with crystalline and quasicrystalline structures can be generated with a collimated light illuminating a mask with multiple apertures regularly distributed on a ring [12]. Therefore,

#195482 - $15.00 USD Received 8 Aug 2013; revised 16 Sep 2013; accepted 17 Sep 2013; published 25 Sep 2013

the input field just after the mask for the pseudonondiffracting beams with crystalline and quasicrystalline structures can be approximately given by

$$E_i(\rho',\phi') = \frac{1}{q}\delta(\rho' - R)\sum_{s=0}^{q-1}\delta\left(\phi' - \frac{2\pi s}{q}\right), \tag{12}$$

where R is the radius of the ring where the apertures are located on. Equation (12) implies that the aperture size must be infinitesimal for generating ideal nondiffracting beams with crystalline structures. For generating nondiffracting superlattice beams, the input field is given by

$$E_i(\rho',\phi') = \frac{\delta(\rho' - R)}{q}\sum_{s=0}^{q-1}\left[\delta\left(\phi' - \frac{2\pi s}{q}\right) + \delta\left(\phi' - \frac{2\pi s}{q} - \Delta_q\right)\right], \tag{13}$$

where Δ_q satisfies the criteria of superlattice patterns in Eq. (6) or (8). However, an infinitesimal aperture is not realistic. Since the aperture sizes cannot be infinitesimal, the generated beams are called the pseudo-nondiffracting beams. Furthermore, the selection of the aperture size determines how many spatial periods can be included in the pseudonondiffracting superlattice beam. Therefore, the analysis for determining the aperture size is of crucial importance. For considering the effect of the aperture size with finite energy, we exploit the multiple Gaussian beams to model the input field just after the apertures. Based on the locations of the pinholes in Eq. (13), the multiple Gaussian waves for describing the input field is given by

$$\begin{aligned} E_i(\rho',\phi') = \left(\frac{2}{\pi\cdot a^2}\right)^{\frac{1}{2}}\sum_{s=0}^{q-1}\Bigg\{&\exp\left[-\frac{\rho'^2 + R^2 - 2\rho' R\cdot\cos\left(\phi' - (2\pi s/q)\right)}{a^2}\right] \\ &+\exp\left[-\frac{\rho'^2 + R^2 - 2\rho' R\cdot\cos\left(\phi' - (2\pi s/q) - \Delta_q\right)}{a^2}\right]\Bigg\}, \end{aligned} \tag{14}$$

where the beam waist of the Gaussian beam is set to be the radius of the aperture a. Since the output field in the focal plane behind the lens can be found by the Fourier transform of the input field, the substitution of Eq. (14) into Eq. (10) and considering $z = f$ lead to an equation for the output field

$$\begin{aligned} E_o(\rho,\phi;f) = &\left(\frac{2}{\pi a^2}\right)^{\frac{1}{2}}\cdot\frac{e^{i\frac{2\pi}{\lambda}(2f)}\cdot e^{\frac{-R^2}{a^2}}}{i\lambda f} \\ &\times\iint e^{\frac{-\rho'^2}{a^2}}\cdot e^{\frac{2R\rho'}{a^2}\cos(\phi-\phi')}\cdot e^{-i\frac{2\pi\rho\rho'}{\lambda f}\cos(\phi-\phi')}\rho' d\rho' d\phi'. \end{aligned} \tag{15}$$

With transformation of coordinates from polar coordinates to Cartesian coordinates, Eq. (15) can be an analytical integration by utilizing Gaussian integral:

$$\int_{-\infty}^{\infty} e^{-\alpha x^2 - 2\beta x}\, dx = \sqrt{\frac{\pi}{\alpha}}\, e^{\beta^2/\alpha}. \tag{16}$$

By some algebraic operation, the output field in polar coordinates can be derived as

$$E_o(\rho,\phi;f) = \frac{\pi a^2 e^{i\frac{2\pi}{\lambda}(2f)} e^{\frac{-\pi a^2}{\lambda f}\rho^2}}{i\lambda f}\cdot\sum_{s=0}^{q-1}\left[e^{-i\frac{2\pi R}{\lambda f}\rho\cos\left(\phi - \frac{2\pi s}{q}\right)} + e^{-i\frac{2\pi R}{\lambda f}\rho\cos\left(\phi - \frac{2\pi s}{q} - \Delta_q\right)}\right]. \tag{17}$$

#195482 - $15.00 USD Received 8 Aug 2013; revised 16 Sep 2013; accepted 17 Sep 2013; published 25 Sep 2013

It can be seen that the terms in the summation represent the superlattice waves with $K = 2\pi R/\lambda f$. The factor of $\exp\left(-\pi a^2\rho^2/\lambda f\right)$ shows that the larger the aperture size, the smaller visible region, namely the less energy in the final beam. Figures 4(a)-4(c) illustrate the numerical patterns for the intensity of the output fields $E_o(\rho,\phi;f)$. It can be seen that more spatial periods can be observed with smaller size of apertures, but it is arduous to generate visible patterns with too small size of apertures in experiments. Thus, the radius of aperture is selected as 85 μm for generating clear pseudonondiffracting optical superlattice patterns.

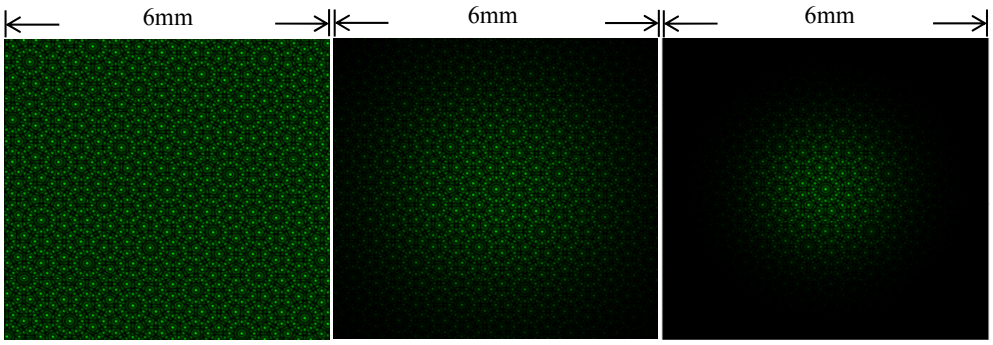

(a) $a \to 0$ (b) $a = 85\mu m$ (c) $a = 120\mu m$

Fig. 4. (a)-(c) Numerically patterns for the output intensity profiles of pseudonondiffracting optical superlattice patterns with different radii of apertures.

Based on the theoretical analysis, an optical configuration is set up to realize pseudonondiffracting optical superlattice patterns, as shown in Fig. 5. The light source was a linearly polarized 20-mW He-Ne laser with central wavelength at 632.8 nm. A beam expander was employed to generate a collimated light and reduce the beam divergence less than 0.1 mrad. By using a laser stencil-cutting machine, we fabricate the steel masks with high precision. The radius of the ring and aperture are 3 mm and 85 μm , respectively. The focal length of the lens is 1000 mm. Interference patterns formed in the region behind the focal lens were imaged by a CCD camera.

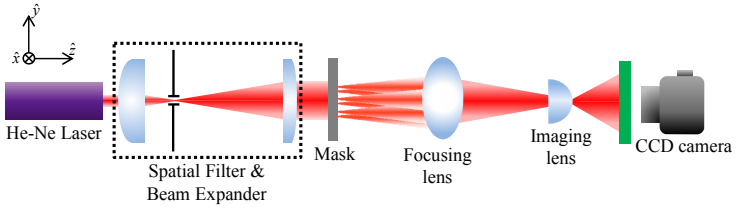

Fig. 5. Experimental setup for generating pseudonondiffracting optical beams with superlattice structures.

Figures 6(a)-6(c) display the interference patterns for pseudonondiffracting optical superlattice structures with q = 4 observed in the experiment under the condition of the optimal alignment. It can be seen that the experimental observations agree very well with the numerical patterns shown in Fig. 2(a)-2(c). The experimental patterns reveal that the relation between the reciprocal lattice constant and the spatial period is satisfied in our theory. Figures 7(a)-7(c) and Figs. 7(d)-7(f) illustrate the experimental results for pseudonondiffracting optical superlattice patterns with q = 3 and 6, respectively. Once again, the experimental results match very well the numerical calculations depicted in Figs. 3(a)-3(c) and Figs. 3(d)-2(f), respectively. It can be experimentally observed that there are honeycomb strucutres in

#195482 - $15.00 USD Received 8 Aug 2013; revised 16 Sep 2013; accepted 17 Sep 2013; published 25 Sep 2013

some optical superlattice pattern with q = 3, as shown in Figs. 7(b) and 7(c). Moreover, in Fig. 7(f), the optical superlattice pattern with q = 6 displays the exotic kaleidoscopic structure. The excellent agreement validates the theoretical analysis of superlattice waves and confirms the experimental approach. The experimental patterns also confirm our analysis of the influence of the aperture size on the transverse unit cell.

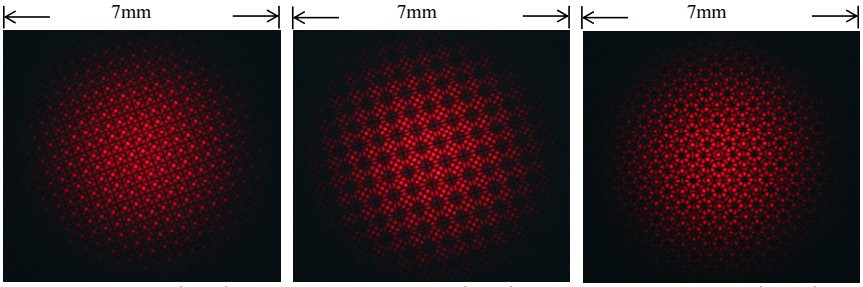

Fig. 6. Experimental patterns observed for pseudonondiffracting optical superlattice beams with q = 4 under the optimal alignment.

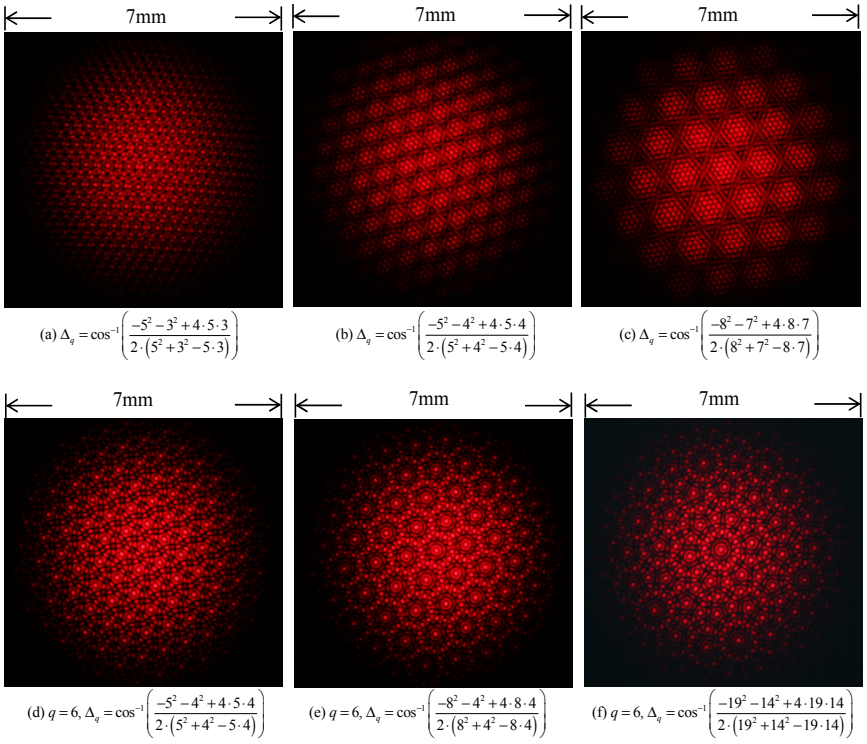

Fig. 7. Experimental patterns observed for pseudonondiffracting optical superlattice beams with (a)-(c) q = 3, and (d)-(f) q = 6.

The reliable generation of optical beams with complex structures has become increasingly important in the studies of optical manipulations. The complex optical fields with the phase singularities, so-called the optical vortex beams, have been extensively employed. For superlattice waves, the phase singularities are the undefined locations in the phase angle fields which are given by

#195482 - $15.00 USD Received 8 Aug 2013; revised 16 Sep 2013; accepted 17 Sep 2013; published 25 Sep 2013

$$\Theta_q\left(\rho,\phi;\vec{K}_s,\Delta_q\right)=\tan^{-1}\left\{\mathrm{Im}\left[\Psi_q\left(\rho,\phi;\vec{K}_s,\Delta_q\right)\right]\Big/\mathrm{Re}\left[\Psi_q\left(\rho,\phi;\vec{K}_s,\Delta_q\right)\right]\right\}, \quad (18)$$

where $\mathrm{Im}\left[\Psi_q\left(\rho,\phi;\vec{K}_s,\Delta_q\right)\right]$ and $\mathrm{Re}\left[\Psi_q\left(\rho,\phi;\vec{K}_s,\Delta_q\right)\right]$ are the imaginary and real parts of the superlattice waves, respectively. Figures 8(a)-8(c) illustrate the contour plots of phase fields $\Theta_q\left(\rho,\phi;\vec{K}_s,\Delta_q\right)$ for Figs. 3(a)-3(c) to display the feature of the phase singularities, respectively. The experimental results verify that the various vortex-lattice structures can be generated by the pseudonondiffracting optical superlattice patterns with $q = 3$.

4. Conclusions

In conclusion, the general conditions of the relative angles for constructing the superlattice waves have been theoretically derived from superposing two identical lattice waves. With the derived formulas, we have numerically presented a variety of superlattice patterns. In order to realize pseudonondiffracting optical beams related to the superlattice structures, we have employed a collimated coherent laser to illuminate a mask with multiple tiny apertures. We have used a stencil laser-cutting machine to fabricate these apertures precisely, and make the positions of the apertures fulfill the conditions for generating superlattice patterns. Considering the realistic patterns, the influence of the aperture size on the number of the transverse unit cells has been also analyzed. The excellent agreement corroborates the theoretical analysis of superlattice waves and supports the experimental configuration for generating pseudonondiffracting optical superlattice beams. Furthermore, the structures of phase singularities for some superlattice patterns have been manifested.

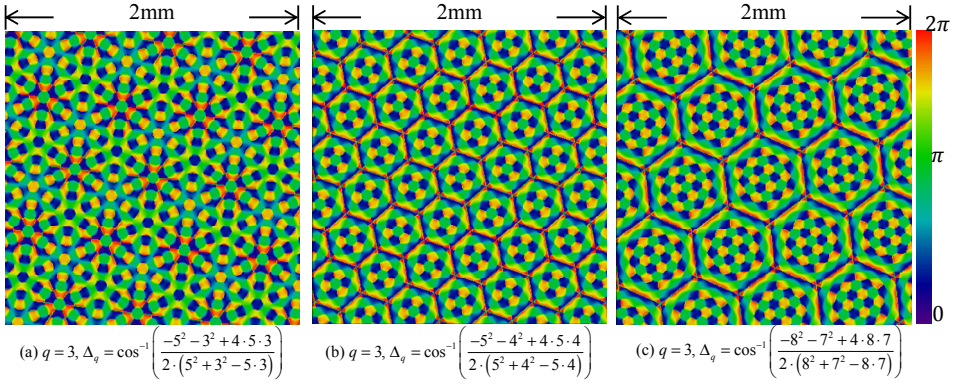

Fig. 8. (a)-(c) Contour plots of phase fields $\Theta_q\left(\rho,\phi;\vec{K}_s,\Delta_q\right)$ for the boxed regions shown in Fig. 3(a)-3(c), respectively.

Acknowledgments

The authors thank the National Science Council for their financial support of this research under Contract No. NSC-100-2628-M-009-001-MY3.

#195482 - $15.00 USD Received 8 Aug 2013; revised 16 Sep 2013; accepted 17 Sep 2013; published 25 Sep 2013